Communication

Formation and Spatio-Temporal Evolution of Periodic Structures in Lipid Bilayers

Sharon Rozovsky, Yoshihisa Kaizuka, and Jay T. Groves

J. Am. Chem. Soc., **2005**, 127 (1), 36-37• DOI: 10.1021/ja046300o • Publication Date (Web): 10 December 2004

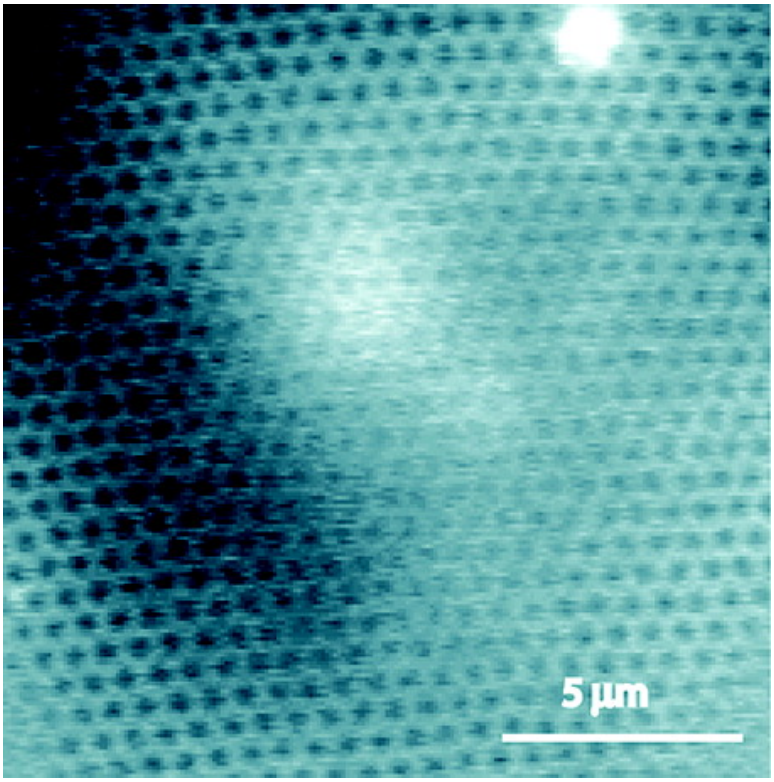

J|A|C|S
COMMUNICATIONS

Published on Web 12/10/2004

Formation and Spatio-Temporal Evolution of Periodic Structures in Lipid Bilayers

Sharon Rozovsky, Yoshihisa Kaizuka, and Jay T. Groves*

Department of Chemistry, University of California, Berkeley, California 94720

Received June 22, 2004; E-mail: JTGroves@lbl.gov

Cell membrane lateral superstructure, particularly organization into large-scale (submicron) domains, is widely implicated in the regulation of protein chemical and biological activity.[1] Miscibility phase separation tendencies are intrinsic to natural lipid/cholesterol mixtures, and these underlying chemical potentials contribute to the free energy landscape within which protein organization occurs. In the following, we describe formation of well-ordered superstructures in phase-separated lipid bilayer membranes. Stripe and hexagonal domain lattices are studied, as well as dynamic transitions between them. Such pattern formation in lipid bilayers is a manifestation of a ubiquitous natural phenomenon, whereby competition between opposing forces results in periodic modulations of an internal order parameter, such as orientation or composition.[2] Relevant examples are the manifold superstructures appearing in lipid monolayers at the air−water interface.[3] Long-range ordering of domains has been noted previously in phase-separated bilayer membranes[4−7] although there is a notable lack of correspondence between the behavior of equivalent lipid mixtures in monolayer and bilayer forms.[8] This indicates differences in the fundamental driving forces governing organization in these systems, and further underscores the need for quantitative measurements on bilayer membranes. The stability and high monodispersity of domain size produced by the methods described here facilitate statistical analysis of spatial distribution functions of the domain lattices. Such analysis is employed to estimate domain interaction forces.

The morphology and dynamics of superstructures in lipid bilayers were monitored in giant unilamellar vesicles (GUVs), composed of an equimolar ternary mixture of sphingomyelin, cholesterol, and dioleoylphosphatidylcholine (DOPC). This composition is widely used as a model raft system based on the constituents of the cell membrane detergent insoluble fraction. Cholesterol and sphingolipids interact favorably, creating a liquid-ordered phase in which mobility is reduced relative to the DOPC-enriched phase. Strong adhesion of closed-form GUVs to a silica substrate, coated with a conventional supported lipid bilayer, leads to asymmetric shapes with relatively high surface area-to-volume ratios,[9] similar to shapes observed previously under thermal expansion and osmotic deflation.[10,11] After adhesion, the bound shape gradually transforms to a lowest-energy shape under the adhesion constraints.[9] Shape changes drive lateral phase separation since local elastic properties and composition are coupled. Stated differently, parameters such as the internal hydrostatic pressure, the membrane lateral tension, and the adhesion area are modified by the conformational changes, and the resulting strain is reduced by adjustment of the superstructure modulation period.

A time series of images depicting a typical stripe to hexagonal lattice superstructure transition is shown in Figure 1. The images were collected by epifluorescence microscopy using a fluorescent dye (Texas Red DPPE), which preferentially partitions into the DOPC-rich phase. In this sequence, phase separation is recorded in the nonadhering region of the vesicle; domain superstructures were not seen in the adhesion zone. Initial phase separation from a homogeneous mixture (Figure 1A) appears as growth of constant width, serpentine stripes composed of a cholesterol/sphingolipid-rich phase; the stripes elongate along the vesicle longitudinal axis. The stripe phase observed here is likely to be fluid based on the frequent occurrence of loops and ripples. As the vesicle shape evolves, the stripe width and spacing are simultaneously reduced (Figure 1B). At the transition (Figure 1B,C), the stripes become unstable and undergo a pearling phenomenon; the stripes acquire a wavy unevenness and bud off uniformly sized circular domains. Interdomain repulsion leads to initial arrangement of the domains into an ordered hexagonal lattice (Figure 1D). That configuration further evolves into a more disordered state (Figure 1E).

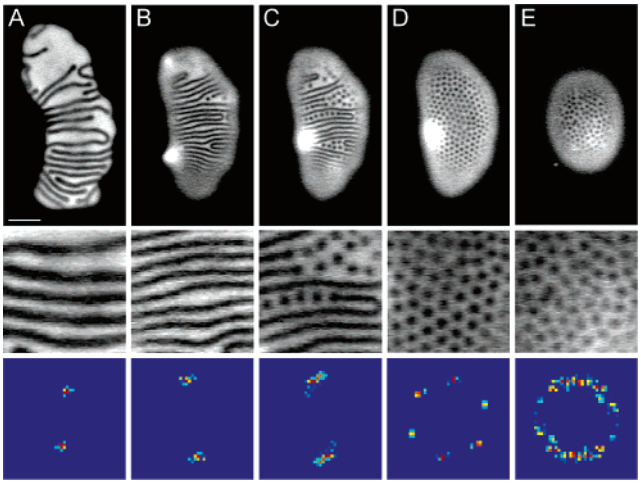

Figure 1. Epifluorescence microscopy images of lateral phase separation in a vesicle adhering to a supported lipid bilayer. An aligned stripe pattern is transformed into a hexagonal array of circular domains as the vesicle shape evolves. Fourier spectra (bottom) are calculated for the ordered regions of interest (middle). The changes in periodicity and radial disorder can be assessed from the distance between the peaks and their width. The respective modulation periods are (A) 1.19 ± 0.05 μm, $t = 0$ s (shortly after adhesion); (B) 0.85 ± 0.05 μm, $t = 528$ s; (C) 0.8 ± 0.1 μm, $t = 596$ s; (D) 0.79 ± 0.05 μm, $t = 648$ s; (E) 0.8 ± 0.1 μm, $t = 1092$ s. The scale bar represents 5 μm.

Another example, presented in Figure 2, demonstrates the evolution of a large circular domain into a stripe superstructure. In these images, the fluorescent dye, cholesteryl BODIPY, partitions into the sphingomyelin-rich phase (Supporting Information). The domain is seen to undergo increasing shape fluctuations, culminating in a fingering process. The initially varied stripes quickly evolve into a highly uniform stripe array. The high connectivity of the stripe phase facilitates shape equilibration since lipid can flow within the phase. The high monodispersity we frequently observe in lattices of circular domains likely stems from their formation from an initially striped superstructure.

10.1021/ja046300o CCC: $30.25

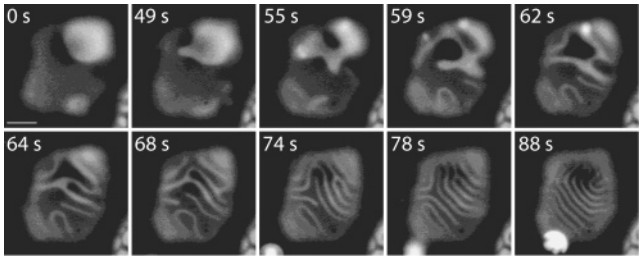

Figure 2. Epifluorescence microscopy images of a circular domain shape instability. The circular domain is transformed into a lower symmetry shape with branched arms, which in turn, develops into a stripe superstructure (t = 0 s is about 2 min after adhesion). The scale bar represents 5 μm.

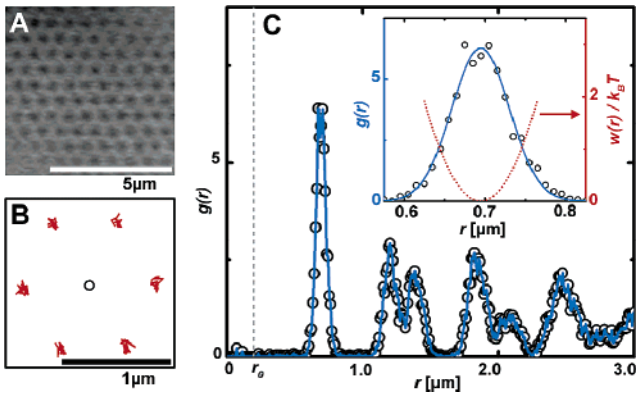

Figure 3. Magnitude of mean force between domains can be estimated from their radial pair distribution function. (A) A representative section of a monodisperse domain lattice. (B) Domain motion, relative to the central domain marked "o", during the trajectory analyzed. (C) Radial pair distribution function (r_0 marks the domain diameter), which is the point at which two domains would come into direct contact. Inset: the first peak in $g(r)$ is enlarged. The dotted red line indicates a parabolic fit of the logarithm of the $g(r)$ first peak, which is the effective potential of mean force, $w(r)$.

Parallel stripes, hexagonal ordering of circular domains, and domain shape instabilities have been observed during phase separation in free floating, fluid bilayers.[6,7] Unique to the domain patterns presented here are their relative stability, prominent symmetry, and high monodispersity of domain size, as well as a correlation between superstructure modulation wavelength and overall vesicle shape. As can be seen in Figure 1, distinct superstructure morphology can exist for many minutes; its overall stability is contingent upon that of the vesicle's shape. Individual hexagonally arranged circular domain lattices, affiliated with hemispherical shapes, were monitored for up to 60 min. Ordered stripes were recorded predominantly in asymmetrically shaped vesicles. The domain boundaries are well defined (strong segregation limit). It is important to note that as adhesion modifies the miscibility phase diagram, the transition temperature or pressure may change during the experiment; the current study was conducted at 25 °C, but patterns were also observed at 20 °C.

Superstructure formation is driven by long-range repulsive interactions between coexisting phases, which oppose the short-range attractions that lead to the phase separation itself. In lipid monolayers at the air−water interface, electrostatic dipole interactions originating from the permanent molecular dipole moments of the lipids provide the dominant repulsive force.[3] Although such electrostatic interactions are significantly screened by the presence of water on both sides of a bilayer membrane, they may still contribute. However, our observations of ordered superstructures at elevated ionic strength (40 mM NaCl) are indicative of contributions from other long-range interaction forces. In bilayers, such long-range interactions could arise from topographical membrane bending. Lateral pressure, resulting from line tension around the boundary of a circular domain, for example, can cause the domain to bend out of the plane of the membrane. As two such domains approach one another, the intervening membrane is forced to bend as well, leading to a repulsive interdomain force. The coupling between composition and local curvature in multicomponent membranes can also modulate the miscibility phase diagram.[12] Accordingly, periodic phase morphologies in lipid bilayers have been theoretically predicted by invoking coupling of local composition to elastic strain.[13]

Highly monodisperse collections of phase-separated domains are of utility for quantitative analysis of membrane physical properties. By tracking the relative positions of domains through a time series of images, one can measure the pair distribution function, $g(r)$, for the array. Analysis of a representative system is depicted in Figure 3. This example consists of ∼200 nm diameter domains configured into a highly ordered hexagonal crystal with ∼700 nm interdomain spacing. Despite the crystalline structure of the domain array, the membrane itself is fluid. The structure is stabilized by interdomain repulsions. A close view of the first peak in $g(r)$ (Figure 3C inset) reveals a Gaussian distribution of interdomain separation distances. This provides a measure of the potential of mean force $\{w(r) = -k_BT \ln[g(r)]\}$, the curvature of which can be interpreted as an effective spring constant for motion of a domain within its hexagonal lattice of nearest neighbors. Various factors, such as polydispersity of domain diameter and image resolution, can broaden the measurement of $g(r)$. Therefore, the effective spring constant determined for this array, 790 $k_BT/\mu m^2$, represents an estimate of interaction forces between domains. Enumeration of the forces governing order and coordination in model membrane domains may enrich our understanding of their organizing principles in biological systems. Last, stabilization of phase-separated membrane superstructures provides a suitable test system for investigations of protein partitioning into and interactions within the various lipid phases.

Acknowledgment. This work was supported by the U.S. Department of Energy under Contract No. DE-AC03-76SF00098. We thank Dr. Sophie Pautot and Dr. Martin Forstner for helpful discussions.

Supporting Information Available: Experimental details and the complete time sequence of all figures. This material is available free of charge via the Internet at http://pubs.acs.org.

References

(1) Vereb, G.; Szollosi, J.; Matko, J.; Nagy, P.; Farkas, T.; Vigh, L.; Matyus, L.; Waldmann, T. A.; Damjanovich, S. *Proc. Natl. Acad. Sci. U.S.A.* **2003**, *100*, 8053−8058.
(2) (2) Seul, M.; Andelman, D. *Science* **1995**, *267*, 476−483.
(3) (3) McConnell, H. M. *Annu. Rev. Phys. Chem.* **1991**, *42*, 171−195.
(4) (4) Krbecek, R.; Gebhardt, C.; Gruler, H.; Sackmann, E. *Biochim. Biophys. Acta* **1979**, *554*, 1−22.
(5) (5) Gebhardt, C.; Gruler, H.; Sackmann, E. Z. *Naturforsch., C: Biosci.* **1977**, *32*, 581−596.
(6) (6) Veatch, S. L.; Keller, S. L. *Biophys. J.* **2003**, *85*, 3074−3083.
(7) (7) Baumgart, T.; Hess, S. T.; Webb, W. W. *Nature* **2003**, *425*, 821−824.
(8) (8) McConnell, H. M.; Vrljic, M. *Annu. Rev. Biophys. Biochem.* **2003**, *32*, 469−492.
(9) (9) Seifert, U. *Adv. Phys.* **1997**, *46*, 13−137.
(10) (10) Kas, J.; Sackmann, E. *Biophys. J.* **1991**, *60*, 825−844.
(11) (11) Lipowsky, R. *Nature* **1991**, *349*, 475−481.
(12) (12) Kawakatsu, T.; Andelman, D.; Kawasaki, K.; Taniguchi, T. *J. Phys. (Paris)* **1993**, *3*, 971−997.
(13) (13) Leibler, S.; Andelman, D. *J. Phys. (Paris)* **1987**, *48*, 2013−2018.

JA046300O